Monitoring Xenon Clathrate Hydrate Formation on Ice Surfaces with Optically Enhanced ^{129}Xe NMR

T. Pietrass,* H. C. Gaede, A. Bifone, A. Pines, and J. A. Ripmeester[†]

Contribution from the Materials Sciences Division, Lawrence Berkeley Laboratory, 1 Cyclotron Road, Berkeley, California 94720, Department of Chemistry, University of California, Berkeley, California 94720, and Steacie Institute for Molecular Sciences, National Research Council of Canada, Ottawa, Ontario KIA OR9, Canada

Received February 1, 1995[⊗]

Abstract: A new technique for monitoring the formation of xenon clathrate hydrates is presented. Under controlled-temperature conditions, clathrate formation is studied with optically enhanced ^{129}Xe NMR spectroscopy, which allows the observation of the xenon occupation of both small and large clathrate cages. The experiments were performed in a temperature range of 170 to 258 K. Only in the range of 195 to 233 K did clathrate formation occur, with applied pressures of typically 0.3 MPa. The NMR data are analyzed with a simple kinetic model, which provides a rate coefficient for clathrate formation and a time constant which describes the decay of the NMR signal intensity. The analysis of the rate coefficients and occupancy ratios of the large to the small cages under the different experimental conditions enabled us to obtain some novel information on the hydrate phase formed on ice surfaces. The results suggest that the surface phase formed initially has many more occupied small cages than the bulk phase at equilibrium and that the composition evolves toward that of the bulk phase in a few minutes. At higher temperatures (258 K) the surface phase seems to be less stable than the bulk phase.

Introduction

Since the discovery of gas hydrates in 1811 by Davy[1] and noble gas hydrates by Villard[2] and de Forcrand,[3] clathrate hydrates have been the subject of intense research. Clathrate hydrates are potentially important for the safe storage and transport of energy.[4] The energy density stored in hydrates is considerably higher than that of conventional natural gas.[5] Recent investigations consider the possibility of disposing industrially produced carbon dioxide as a hydrate in deep ocean to prevent further release into the atmosphere as greenhouse gas.[6] Clathrate formation can be a nuisance, however, as hydrate plugs in offshore oil wells and pipelines for transport of unprocessed fluids present a problem of high economic impact. The ability to stimulate and inhibit clathrate formation depends on a detailed understanding of the clathrate formation mechanism.

Xenon serves as a good model for methane with respect to size and shape. Xenon also forms a clathrate hydrate with water, the structure of which consists of six larger tetrakaidecahedral and two smaller pentagonal dodecahedral cages per unit cell. The free diameter of the larger cages is 0.59 nm, that of the smaller cages 0.52 nm, resulting in a maximum of eight xenon atoms (diameter 0.44 nm) per unit cell, with one xenon atom residing in each cage.[7] For the purpose of NMR investigations, xenon is a more favorable nucleus than carbon due to the high polarizability of its electron cloud and the resulting large chemical shift range. Ripmeester and Davidson[8] first introduced ^{129}Xe NMR to study cavities in xenon deuterohydrate. Ito and Fraissard[9] extended the application to probe cavities in zeolites. In anisotropic cavities,[10] Ripmeester and co-workers were able to differentiate between structure I, stucture II, and structure H clathrate hydrates[11] because the ^{129}Xe chemical shift is a function of the cage space available to the xenon.[12,13] The major drawback of this technique is the occurrence of long spin lattice relaxation times for ^{129}Xe in clathrate hydrates (on the order of minutes[14]) which prohibits the study of non-equilibrium samples. It is possible to decrease the acquisition time from 4 h (at 275 K) to 24 min (at 265 K) by using proton to xenon cross polarization.[15] However, as the xenon clathrate hydrate formation occurs on the time scale of minutes,[16] it is still not possible to monitor the uptake of the xenon by conventional ^{129}Xe NMR spectroscopy. The kinetics of the clathrate formation have been previously studied by a volumetric method,[16,17] a technique which does not give information on a molecular scale. It is therefore of interest to look for evidence of precursor structures or other evidence of nonequilibrium behavior. As the equilibrium occupancy ratios [large cage/small cage] often differ substantially from the stoichiometrical value of three, even after long equilibration times,[14] it is of particular interest to follow the occupancies of two distinct cages.

Conventional ^{129}Xe NMR is a useful tool for monitoring the

* Address correspondence to this author at Université Louis Pasteur, Institut Le Bel, 4 rue Blaise Pascal, F-67070 Strasbourg, Cedex, France.
  † Steacie Institute for Molecular Sciences.
  ⊗ Abstract published in *Advance ACS Abstracts,* June 1, 1995.
  (1) Davy, H. *Phil. Trans. R. Soc. (London)* **1811,** *101,* 1.
  (2) Villard, P. C. R. *Hebd. Séances Acad. Sci.* **1896,** *123,* 377.
  (3) de Forcrand, R. C. R. *Hebd. Séances Acad. Sci.* **1923,** *176,* 335.
  (4) Teal, A. G.; Westerman, J. F.; Ott, V. J. U.S. Patent 4821794, Apr. 18, **1989.**
  (5) McDonald, G. T. *Annu. Rev. Energy* **1990,** *15,* 53.
  (6) Englezos, P.; Hatzikiriakos, S. G. *Ann. N.Y. Acad. Sci.* **1994,** *715,* 270.
  (7) (a) v. Stackelberg, M.; Müller, H. R. *Naturwissenschaften* **1975,** *39,* 20. (b) Claussen, W. F. *J. Chem. Phys.* **1951,** *19,* 1425. (c) Pauling, L.; Marsh, R. E. *Proc. Natl. Acad. Sci. U.S.A.* **1952,** *38,* 112.

  (8) Ripmeester, J. A.; Davidson, D. W. *Bull. Magn. Reson.* **1981,** *2,* 139.
  (9) Ito, T.; Fraissard, J. *J. Chem. Phys.* **1982,** *76,* 5225.
  (10) Lee, F.; Gabe, E.; Tse, J. S.; Ripmeester, J. A. *J. Am. Chem. Soc.* **1988,** *110,* 6014.
  (11) Ripmeester, J. A.; Ratcliffe, C. I. *J. Phys. Chem.* **1990,** *94,* 8773.
  (12) Ripmeester, J. A.; Ratcliffe, C. I.; Tse, J. S. *J. Chem. Soc., Faraday Trans. 1* **1988,** *84,* 3731.
  (13) Cheung, T. T. P. *J. Phys. Chem.* **1992,** *96,* 5505.
  (14) Ripmeester, J. A.; Davidson, D. W. *J. Mol. Struct.* **1981,** *75,* 67.
  (15) Davidson, D. W.; Handa, Y. P.; Ripmeester, J. A. *J. Phys. Chem.* **1986,** *90,* 6549.
  (16) Barrer, R. M.; Edge, A. V. J. *Proc. R. Soc. (London)* **1967,** *A 300,* 1.
  (17) Sloan, Jr., E. D.; Fleyfel, F. *AIChE J.* **1991,** *37,* 1281.

[129]Xe *NMR Study of Clathrate Formation*

J. Am. Chem. Soc., Vol. 117, No. 28, 1995 7521

occupancy of each cage size, but its sensitivity is far too low to detect signals on the time scale required to study clathrate formation. The use of optically polarized xenon, however, allows the signal detection following a single radio frequency pulse with sufficient sensitivity.[18] Typically, a sensitivity enhancement of a factor of 10^4 to 10^5 is achieved over conventional [129]Xe NMR, so that the acquisition time for each spectrum is reduced to a single scan, which takes typically a few milliseconds. In this work, we report a [129]Xe NMR study of the formation of xenon clathrate hydrates using highly spin-polarized xenon.
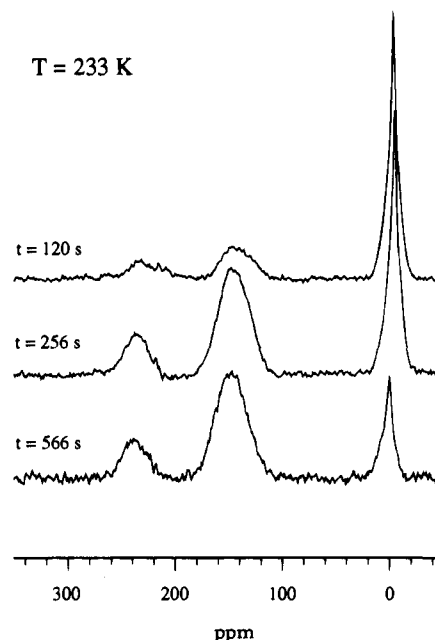
Experimental Section

The experiments utilized a home-built low-temperature NMR probe equipped with a saddle coil and operating at a Larmor frequency of 100.277 MHz for [129]Xe. The 90° pulse length was 14 μs; a pulse length of 8 μs was applied in the experiments. Cooling of the probe was achieved with a flow of cold nitrogen gas to the dewared sample region.

Highly polarized xenon was produced via spin exchange with rubidium atoms in the gas phase, a process described in detail elsewhere.[19] The rubidium was irradiated on resonance with the rubidium D_1 line with 1.2−1.5 W of circularly polarized light for 30−60 min. A CW titanium sapphire ring laser (Schwartz Electro Optics) pumped by an argon ion laser (Coherent Laser Group) was used as the light source. The irradiation time was dictated not by the attainable xenon polarization (estimated to be on the order of 10−20%) which is reached typically after 30 min, but by experimental procedures such as sample preparation and equilibration. The optical pumping cell was located in a magnetic field of 30 G provided by a pair of Helmholtz coils. The magnetic field axis was parallel to the propagation vector of the light.

The sample consisted of ice prepared by dripping D_2O (Aldrich) in liquid nitrogen, which was then ground up in a mortar and quickly transferred into the NMR sample tube which was cooled and immediately evacuated to minimize the amount of included oxygen. The sample was equilibrated for at least 1 h in a slush bath prior to addition of the xenon (EG&G Mound, 80% enriched in [129]Xe and depleted to 2% in [131]Xe). A 10-mm NMR tube equipped with a high-vacuum stopcock and a sidearm for the xenon served as a sample tube. The sidearm was kept at ambient temperature during the equilibration of the ice. Equilibration temperatures were 258, 233, 217, 195, and 170 K.

Prior to the NMR experiment, the sidearm of the sample tube was immersed in liquid nitrogen in order to freeze the optically pumped xenon from the optical pumping cell into the sidearm. The amount of xenon varied in the different experiments. The pumping cell was loaded with 337 Torr of xenon at 258 K, 305 Torr at 233 K, 64 Torr at 217 K, 281 Torr at 195 K, and 280 Torr at 170 K. Pressures were measured at ambient temperatures. During the freezing procedure, the sample tube was maintained in a magnetic field of 100 G, also provided by a pair of Helmholtz coils, to slow down the xenon relaxation.[20] After the xenon was frozen, the sample tube was transferred to the high-field NMR magnet (8.52 T) for detection, where the probe was precooled to the same temperature as the sample. The transfer of the sample tube to high field was normally accomplished in 5 s.

Following the NMR experiments, the xenon was recovered by connecting the sample tube to the vacuum line and immersing the sample region in a bath of dry ice/ethanol. It is important to note that merely opening the sample tube to the vacuum led to only a partial release of the xenon; complete recovery could only be achieved after warming up the ice to free the enclathrated xenon. Selective freezing

(18) Raftery, D.; Long, H.; Meersmann, T.; Grandinetti, P. J.; Reven, L.; Pines, A. *Phys. Rev. Lett.* **1991**, *66*, 584.

(19) (a) Kastler, A. *J. Phys. Radium* **1950**, *11*, 255. (b) Bouchiat, M. A.; Carver, T. R.; Varnum, C. N. *Phys. Rev. Lett.* **1960**, *5*, 373. (c) Bhaskar, N. D.; Happer, W.; McClelland, T. *Phys. Rev. Lett.* **1982**, *49*, 25. (d) Bhaskar, N. D.; Happer, W.; Larsson, M.; Zeng, X. *Phys. Rev. Lett.* **1983**, *50*, 105. (e) Happer, W.; Miron, E.; Schaefer, S.; Schreiber, D.; Wijngaarden, W. A. v.; Zeng, X. *Phys. Rev. A* **1984**, *29*, 3092.

(20) Gatzke, M.; Cates, G. D.; Driehuys, B.; Fox, D.; Happer, W.; Saam, B. *Phys. Rev. Lett.* **1993**, *70*, 690.

Figure 1. [129]Xe NMR spectra of the formation of a xenon clathrate hydrate at 233 K and time *t* after admission of the xenon to the powdered ice sample.
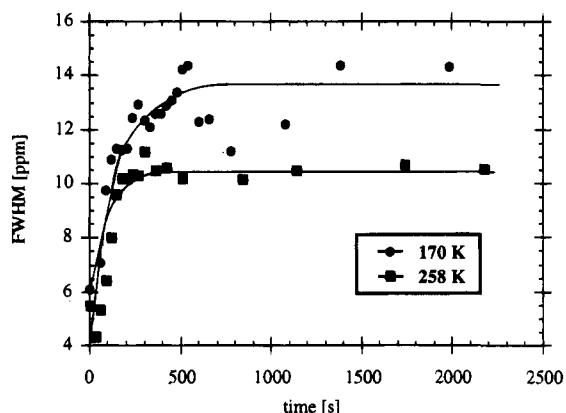
Figure 2. [129]Xe NMR line width (full width at half maximum, fwhm) of xenon gas in the presence of powdered ice as a function of time after the admission of the xenon at different temperatures. The curves serve as a guide to the eye.

of the water in the ethanol bath allows xenon recovery, because freezing of water in the presence of xenon (at the reported pressures) only causes clathrate formation upon agitation.[21]

Results and Discussion

Figure 1 shows three typical [129]Xe NMR single-scan spectra obtained at different times *t* elapsed after insertion of the sample into the magnet. The gas peak is referenced to 0 ppm. Extrapolation to zero pressure[22] would result in a shift of +1.5 ppm which is not relevant in the subsequent analysis. The signal at 160 ppm is attributed to xenon in the larger tetrakaidecahedral cages, and the one at 240 ppm is attributed to xenon in the smaller dodecahedral cages.[14] Instead of observing the expected narrow line shape of the gas signal (<0.25 ppm) we observe a broad signal, whose line width is dependent on both temperature and the time the xenon spent in the sample tube (Figure 2). The steep increase of the line width in the first 200 s is very
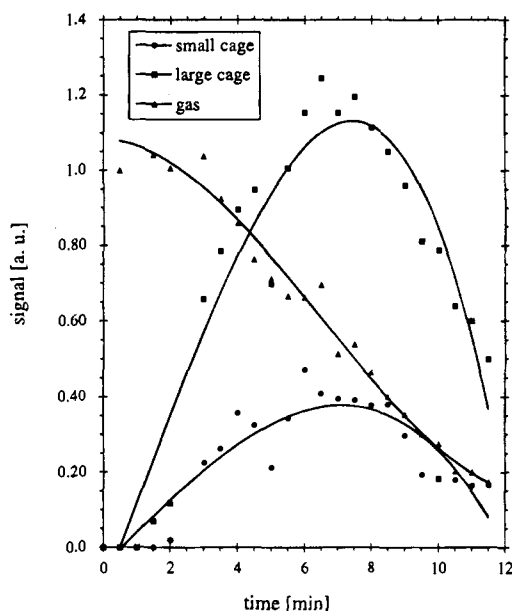
(21) Pietrass, T.; Bowers, C. R.; Gaede, H. C.; Bifone, A.; Pines, A.; unpublished results.

(22) Jameson, D. J.; Jameson, A. K.; Cohen, S. M. *J. Chem. Phys.* **1973**, *59*, 4540.

Figure 3. Formation of a xenon clathrate hydrate at 217 K monitored by the change in the integrated intensities of the ^{129}Xe NMR signals with time t after admission of the xenon. The curves serve merely to guide the eye.

likely due to xenon subliming in the sidearm of the sample tube, as the xenon was transferred to the magnet while frozen. This is consistent with the observation that the gas signal intensity first *increases* with time. Only about 20% of the total sample tube volume is located in the dewared region of the probe. This creates a small temperature and pressure gradient in the sample tube, which contributes to the line width. It is reported that a xenon gas sample of comparable density experienced a shift of 4 ppm when the temperature is changed from 250 to 300 K.[22] Furthermore, the gas signal is the sum of the signal of xenon gas inside *and* outside the pickup coil, due to the high polarization. Xenon in the void spaces close to the surface of the ice crystals might experience a different susceptibility from xenon in the free gas space, so the line width may also be due to susceptibility broadening. It is pertinent to emphasize that the three resonances assigned to xenon in the small cage, large cage, and gas phase were the only ones observed.

The spectra were analyzed by integrating the signals and plotting the values as a function of time. The formation of the xenon clathrate hydrates at 217 K is shown in Figure 3. The time axis in Figure 3 terminates at $t = 12$ min although the experiment was performed over a time scale of 43 min. At times $t > 12$ min, the (larger) peak of the xenon in the large cages as well as the gas signal can still be observed, but the signal-to-noise ratio decreased, prohibiting reliable data analysis.

The onset of clathrate formation is delayed by 1.5 min after inserting the sample tube in the magnet. In this period of time, the frozen xenon warms up until the pressure has reached at least the dissociation pressure of the clathrate at the prevailing temperature. A rapid increase in the xenon pressure in the first minutes is consistent with the steep increase in the line width of the gas signal. The dissociation pressures[23] and the initial xenon pressures are listed in Table 1. Although water was present in stoichiometric excess with respect to xenon, and the xenon pressure decreased during each experiment due to enclathration, it is known that the xenon forms a clathrate layer on the surface of the ice crystal, which is impenetrable by the xenon.[24] Therefore, we assume that excess xenon was available

Table 1. Xenon Clathrate Hydrate Dissociation Pressures P_{diss} (from ref 23) and Initial Xenon Pressures P_0 (Calculated for Room Temperature) Used in the NMR Experiments[a]

	T (K)				
	170	195	217	233	258
P_{diss} (10^5 Pa)	0.004	0.045	0.16	0.27	0.78
P_0 (10^5 Pa)	2.62	2.62	0.60	2.85	2.85

[a] P_{diss} and P_0 are listed for the temperatures T at which the experiments were performed.

throughout the experiments. The permanent presence of the xenon gas signal in the spectra supports this assumption as well as the fact that the sample tubes were still pressurized when they were opened for xenon recovery.

To determine the kinetics of the reaction, a model for the reaction mechanism is required. Bishnoi and co-workers[25] formulated a semiempirical model to correlate their experimental data, which were obtained by contacting methane with water upon vigorous stirring. The rate of hydrate formation is dependent on the supersaturation of the liquid water, a situation which is not comparable to ours. Holder and co-workers[26] used an experimental design with a fixed gas—water or gas—ice interfacial area. Initially, their experiments were carried out at 263 K using gas pressures as high as 12 MPa. However, they only observed clathrate formation when warming the gas temperature above the melting point of ice, which led to the conclusion that melting ice provides a template for hydrate nucleation. We observed hydrate formation at temperatures as low as 195 K at a gas pressure of only 0.3 MPa, conditions which exclude the presence of liquid water. Sloan and Fleyfel[17] proposed a molecular mechanism for gas hydrate nucleation from ice, to our knowledge the only work in the literature which deals with the nucleation period and not the crystal growth regime. The authors modeled Falabella's data,[27] which show that for the formation of xenon clathrate hydrate from ice there is no induction period, a result consistent with our data and those of Barrer and Edge.[16] Sloan and Fleyfel propose a mechanism which involves the presence of transient liquid water on a local scale, since the formation of one cavity requires the relocation of 20 ice lattice molecules. Falabella used a shaking ball-mill apparatus similar to the one of Barrer and Edge. The impinging balls on the ice/hydrate surface provide sufficient mechanical energy to form liquid water locally even at low temperatures.[17] However, as indicated above, our data suggest that the presence of transient liquid water is not a necessary condition for hydrate formation.

The formation of clathrate hydrates in the absence of transient liquid water has been previously observed. Taking an adsorption isotherm of carbon oxide on ice, Adamson and Jones[28] observed at 195 K at a vapor pressure only half of the equilibrium pressure of the liquid carbon dioxide a steep increase in the gas uptake which they attributed to clathrate formation. Hallbrucker and Mayer[29] found under similarly mild experimental conditions (guest pressures of 1 bar and temperatures around 200 K) unexpectedly stable clathrate hydrates of oxygen, nitrogen, carbon monoxide, and argon. Fleyfel and Devlin[30]

(23) Tanaka, H.; Nakanishi, K. *Mol. Simul.* **1994**, *12*, 317.

(24) Barrer, R. M.; Ruzicka, D. J. *Trans. Faraday. Soc.* **1962**, *58*, 2262.

(25) Vysniauskas, A; Bishnoi, P. R. *Chem. Eng. Sci.* **1983**, *38*, 1061.

(26) (a) Hwang, M. H.; Wright, D. A.; Kapur, A.; Holder, G. D. *J. Inclusion Phenom.* **1990**, *8*, 103. (b) Holder, G. D.; Zele, S.; Enick, R.; LeBlond, C. *Ann. N.Y. Acad. Sci.* **1994**, *715*, 345.

(27) Falabella, B. J. Ph.D. Thesis, University of Massachussetts, Amherst, MA, 1975.

(28) Adamson, A. W.; Jones. B. R. *J. Colloid Interface Sci.* **1971**, *37*, 831.

(29) Hallbrucker, A.; Mayer, E. *J. Chem. Soc., Faraday Trans.* **1990**, *86*, 3785.

(30) Fleyfel, F.; Devlin, J. P. *J. Phys. Chem.* **1988**, *92*, 631.

[129]Xe NMR Study of Clathrate Formation

J. Am. Chem. Soc., Vol. 117, No. 28, 1995 7523

showed that clathrates of trimethylene oxide, ethylene oxide/carbon dioxide, and ethylene oxide/trimethylene oxide can be formed by epitaxial growth in the temperature range 100–140 K.

The high sensitivity of the optically pumped xenon detection method compared to the volumetric methods discussed above makes it possible to observe hydrate formation on a much smaller scale. Whereas Falabella's data are reported in percent conversion,[17] we are able to observe clathrate formation in the ppm conversion range. For this estimate, we assume that the total amount of ice used in our experiments is converted into an empty structure I hydrate lattice. With the optical pumping enhancement, a detection sensitivity of one occupied cage in 10^6 empty cages is obtained.

A simple model was used to describe the kinetics of hydrate formation in our experimental setup. There is general agreement in the literature that hydrate formation can be divided into two basic steps. In the first step, the gas is adsorbed onto the ice surface, accompanied by a relocation of the ice lattice molecules. The adsorption of the xenon is a reversible process which can occur at any xenon pressure. We refer to this intermediate structure as Xe_{ads}. We assume that the amount of ice converted into clathrate is very small compared to the initial amount of ice present, since we do not use a mechanical device to destroy the impenetrable clathrate layer covering the ice surface.[24] In the second step, the intermediate phase Xe_{ads} converts irreversibly into the clathrate hydrate lattice structure, referred to as Xe_{Clath}. We assume that a minimum number of adsorbed xenon atoms is required for nucleation. The conversion of Xe_{ads} into Xe_{Clath} occurs when this critical number is reached. The concentration of Xe_{ads} is assumed to be constant and Xe_{Clath} depends only on the xenon pressure [Xe]. The rate coefficients for the individual steps cannot be determined from our data and are therefore expressed as an effective rate coefficient K. The processes can be described by the following scheme:

$$Xe \underset{k_d}{\overset{k_{ads}}{\rightleftharpoons}} Xe_{ads}$$
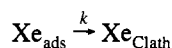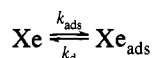
$$Xe_{ads} \overset{k}{\rightarrow} Xe_{Clath}$$

$$\frac{d[Xe_{ads}]}{dt} = 0; \quad [Xe_{ads}] = \frac{k_{ads}}{k + k_d}[Xe] \quad (1)$$

$$\frac{d[Xe_{Clath}]}{dt} = k[Xe_{ads}] = \frac{kk_{ads}}{k + k_d}[Xe] = K[Xe] \quad (2)$$

The clathrate concentration is proportional to the integrated signal intensity of the NMR resonances from the small and large cages. However, it is necessary to account for the fact that the ^{129}Xe NMR signal intensity decays with time due to spin lattice relaxation and, in particular, due to the NMR rf pulses. The correction for the decay due to rf pulses is required because the initial polarization is not the equilibrium Curie law polarization, but is created by the optical pumping process. Both effects are expressed as an overall time constant T_{kill}. Integration of eq 2 and addition of an exponential decay term depending on the time constant T_{kill} yields the fitting function (3)

$$M(t) = Kt[Xe] \exp\left[-\frac{t}{T_{kill}}\right] \quad (3)$$

where $M(t)$ is the time-dependent integrated intensity of the signal of the enclathrated xenon in the large and small cages. Results of the fits are shown in Figure 4; the fitting parameters
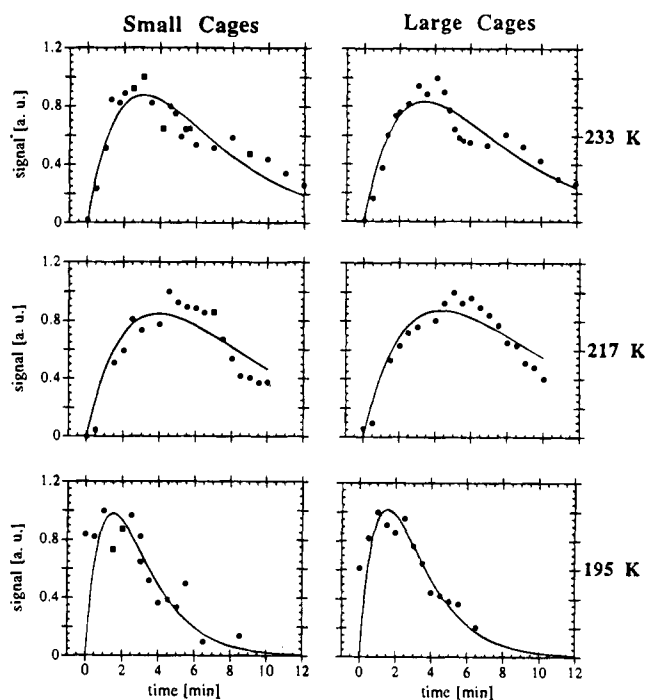
Figure 4. Experimental data points (dots), determined from the ^{129}Xe NMR spectra, approximated by the model function (line) for the large and the small cages at the given temperatures (see text).

Table 2. Rate Coefficients K and Decay Constants T_{kill} for the Formation of Xenon Clathrate Hydrates, Determined for Inclusion of Xenon in the Large and in the Small Cages[a]

T (K)	cage	K	ΔK	T_{kill} (min)	ΔT_{kill} (min)	R
195	large	0.69	0.12	1.54	0.16	0.74
	small	0.68	0.16	1.49	0.20	0.65
217	large	0.91	0.07	4.34	0.25	0.94
	small	0.97	0.10	3.95	0.28	0.92
233	large	0.23	0.02	3.40	0.17	0.94
	small	0.27	0.02	3.07	0.16	0.91

[a] K and T_{kill} are listed for the temperatures at which clathrate formation was observed. R is the correlation coefficient of the fits.

are summarized in Table 2. The time axes in Figure 4 were shifted by −1.5 min to account for the warming up period of the xenon frozen in the sidearm as discussed above. Contrary to the time axis in Figure 3, where $t = 0$ corresponds to the insertion of the sample in the magnet, $t = 0$ in Figure 4 corresponds to the first NMR observation of a clathrate peak. The errors of the fits listed in Table 2 are due to a decrease in signal-to-noise ratio with time and severe phase and baseline correction, which are necessary for integration. The phase of the spectrum is distorted because transverse magnetization which has not decayed will, following a subsequent rf pulse, acquire a different phase from magnetization which is stored along the $+z$ axis.

The data for the rate coefficients K in Table 2 reveal a temperature and pressure dependence. The rate decreases with increasing temperature, a result indicative of a negative activation energy. A negative Arrhenius energy has been experimentally observed previously[25] and has been recently theoretically confirmed.[23] At 217 K, the rate seems faster than at 195 K, but at 217 K the initial xenon pressure was substantially lower than in the other runs, thus raising the value of K in the applied model.

In Figure 5, the ratios of the rate coefficients of the large to the small cages are plotted versus temperature. These ratios are independent of pressure and unknown parameters, such as the volume of the void spaces between ice crystals and the
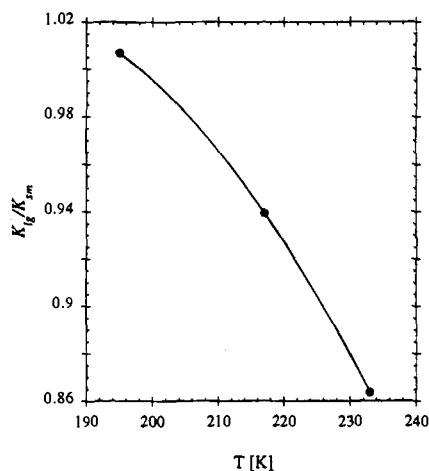
Figure 5. Temperature dependence of the ratios of the rate coefficients for the large over the small cages from Table 2. The curve serves as a guide to the eye.
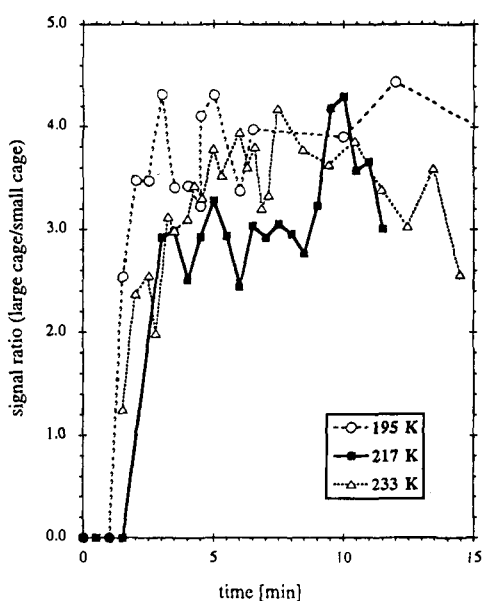
Figure 6. ^{129}Xe NMR signal ratios of xenon in the large to the small cages as a function of time after admission of the xenon.

penetration depth of the xenon into the ice, and should depend only on temperature. With increasing temperature, the smaller cages are occupied more rapidly than the larger cages. Since the ease of clathrate formation decreases with increasing temperature, this may indicate that the intermediate phase Xe_{ads} resembles the smaller cage structure. This result is supported by comparing the individual occupancy ratios of the cages for the various temperatures (Figure 6). Due to the difficulties in phasing the NMR spectra mentioned earlier, the individual cage ratios cannot be determined to better than ±10%, but two general trends can be observed. First, the ratios of the cage occupancies have reached their equilibrium value after a short time (1 to 2 min). The observed equilibrium values of the ratios range for the higher pressure samples (at 195 and 233 K) from about 3.8 to 3.9, consistent with the value obtained by Ripmeester for a well-equilibrated sample.[13] Secondly, the ratios are lower at 217 K where the xenon pressure was also considerably lower compared to that at the other temperatures. It is likely that at this lower pressure, the conversion from the Xe_{ads} phase to the clathrate hydrate structure Xe_{Clath} is incomplete. This is again consistent with the first data points in Figure 6 at 233 and 195 K, which exhibit a considerably smaller ratio of the cage occupancy, until the equilibrium value is reached.

The decay constant T_{kill} listed in Table 2 is the same within experimental error for the small and the large cages. The effect of one pulse is evidently the same for the xenon in both the large and the small cages. The spin lattice relaxation time T_1 of xenon occluded in the two cage types has not been explicitly determined yet, and our results suggest that it is the same for both cages. The xenon spin lattice relaxation time in the gas phase increases with decreasing pressure[31] and decreasing temperature.[32] Since in our experiments the majority of the xenon is in the gas phase and about 80% of the volume of the sample tube is at ambient temperature, the pressure effect on the xenon relaxation should dominate over the temperature effect. At the lowest pressure at 217 K, we therefore expect the longest spin lattice relaxation time, which is in agreement with our results. At the lowest temperature, we observe the shortest decay constant T_{kill}. Since it is primarily the xenon in the coil region which is depolarized by rf pulses, i.e., the enclathrated xenon, the destruction of the polarization is most efficient for the fastest enclathration process at 195 K, which is in agreement with our data.

At 170 and 258 K no clathrate formation could be observed. At the lowest temperature (170 K), the formation of liquid xenon occurred after about 10 min. It has been observed earlier that the condensation of xenon in porous systems is not instantaneous.[33] The liquid xenon was identified by its narrow ^{129}Xe NMR resonance at 240 ppm. At the highest temperature, 258 K, an interesting effect was observed. Following a period of 36.3 min at 258 K without observable clathrate formation, the sample was cooled rapidly from 258 to 231 K and allowed to equilibrate for 10.4 min. The spectrum at $t = 46.7$ min revealed the two signals for enclathrated xenon and the gas signal. The formation of the clathrates was monitored for 17.2 min at 231 K with a spectrum recorded every 2 min, indicating a slight increase in the magnitude of the clathrate peaks. At $t = 63.9$ min the sample was rapidly warmed to 258 K. The spectrum recorded 2 min later revealed only the gas signal with complete disappearance of the two clathrate signals even in absence of sample equilibration. However, Hallbrucker and Mayer[29] observed that in clathrates formed from amorphous solid water, decompositon occurs only close to the melting point of ice, a temperature much higher than the estimated decomposition temperature. The authors conclude that at the elevated temperature the trapped guest provides a pressure high enough to ensure clathrate stability. Upon heating, the clathrate hydrates are protected from dissociation by the same layer of crystalline ice that enabled the pressure buildup of the guest species.[29] These results suggest that in the short exposition time applied in our experiment, only a thin surface layer of clathrate hydrates formed which is subject to melting upon heating. Moreover, thin layers of clathrate hydrates may possess an inherent lower stability than bulk hydrate.

Some comments are in order on the applicability and limits of the experiments as carried out in this work. One aspect that is clearly important is that of quantification. One can assume that initially the magnetizations actually reflect the species in a quantitative way until a reaction occurs, or until a pulse is applied. After this, the magnetizations decay due to application of pulses and natural relaxation processes. Ideally, the pulse lengths should have been short in order to minimize this perturbation due to rf pulses; however, the longer pulse length was dictated by the need for obtaining a signal of sufficient

(31) (a) Torrey, H. C. *Phys. Rev.* **1963**, *130*, 2306. (b) Hunt, E. R.; Carr, H. Y. *Phys. Rev.* **1963**, *130*, 2302. (c) Streever, R. L.; Carr, H. Y. *Phys. Rev.* **1961**, *121*, 20.

(32) Streever, R. L.; Carr, H. Y. *Phys. Rev.* **1961**, *121*, 20.

(33) Ripmeester, J. A. Unpublished results.

amplitude throughout the duration of the experiment (ca. 15 min). In a uniform sample of xenon gas at constant temperature, the magnetization decay due to an rf pulse train (constant pulse angle, uniform pulse spacing) can be evaluated quantitatively, and this fits an exponential function quite well. In our study, however, the temperature was an experimental variable, and there were small temperature and pressure gradients in the sample tube. Also, after some reaction of the xenon gas has occurred, the magnetization of the enclathrated gas and the external gas evolve in different ways. We think quantification problems were minimized by applying a (constant pulse angle, uniform pulse spacing) rf pulse train to the sample, and accounting for the different decay factors empirically. Clearly, it would take considerable effort to disentangle the various mechanisms which contribute to the magnetization decay, especially since these can be expected to be functions of temperature and pressure.

Various experiments could be considered to improve the quantification, e.g. a point-by-point method where each point on the growth curve is taken for a fresh sample from data taken with a single pulse. However, this aproach not only is time consuming but brings its own problems as it requires careful control of starting conditions such as gas pressure and surface area of the ice. Another approach would be to increase the ice surface area by going to vapor-deposited ice, and thus increase the signal from reacting xenon. It should then be possible to go to a much shorter pulse length, and thus reduce the effect of magnetization decay due to rf pulses.

Conclusions

The reaction of xenon gas with an ice Ih surface was followed at a molecular level by optically enhanced ^{129}Xe NMR spectroscopy. The high detection sensitivity of this approach,

when compared to volumetric methods, allowed the observation of clathrate formation at an early stage. Previous results, the absence of an induction period, and a negative Arrhenius energy for the formation process agree with our data.

Our results imply that the mobility of the water molecules must be high enough to organize themselves around the xenon atoms even in the absence of transient liquid water. At higher temperatures, there are indications that the hydrate phase which forms on the surface does not have the same composition or stability as the bulk phase.

After initial exposure of the surface to the xenon, the xenon NMR spectrum shows that there are many more small xenon-filled cages than expected from the stoichiometry of the bulk phase prepared under equilibrium conditions. The cage occupancy ratio evolves with time until the ratio approaches that characteristic of the bulk hydrate. The pressure, temperature, and time dependence of the occupancy ratios of the large over the small cages and of the ratios of the rate coefficients suggest that the intermediate phase, in which xenon is adsorbed onto the ice and has not yet converted into the clathrate hydrate structure, may resemble the structure of the smaller cages.

JA9503488